

Synthesis of mesoporous SiO₂-CeO₂ hybrid nanostructures with high catalytic activity for transamidation reaction

Manu Sharma^{a*}, Harikrishnan K^a, Umesh Kumar Gaur^{b*}, Ashok K. Ganguli^c

^a*Central University of Gujarat, Gandhinagar, India*

^b*VP & RPTP Science College, Vallabh Nagar, India*

^c*Indian Institute of Technology Delhi, New Delhi, India*

**Corresponding author*

FTIR spectra of CeO₂, SiO₂, and the nanocomposite of CeO₂ and SiO₂ are given in Fig. S1, S2, and S3 respectively. Fig. S1 shows the wide band around the region of 3412 cm⁻¹ which is accredited to -OH stretching vibrations and the band position near 1635 cm⁻¹ belongs to H-O-H bending of residual water. The peak around 851 cm⁻¹ is due to the Ce-O-Ce stretching vibrations¹. In Fig. S2, the broad band around 3435 cm⁻¹ is due to -OH stretching vibrations. The signal at 1635 cm⁻¹ is assigned to hydroxyl groups present at the surface of mesoporous silica². The band corresponding to 802 cm⁻¹ and 467 cm⁻¹ were assigned to Si-O-Si symmetric stretching and bending vibrations respectively^{3,4}. In Fig. S3, the plot of the SiO₂-CeO₂ composite shows the band position corresponding to 1384 cm⁻¹ representing Ce-O-Ce vibrations. Also, the peaks at 1006 cm⁻¹ and 464 cm⁻¹ in the composite spectra represent the Si-O-Si stretching and bending vibrations respectively and confirm the presence of both silica and ceria in the composite.

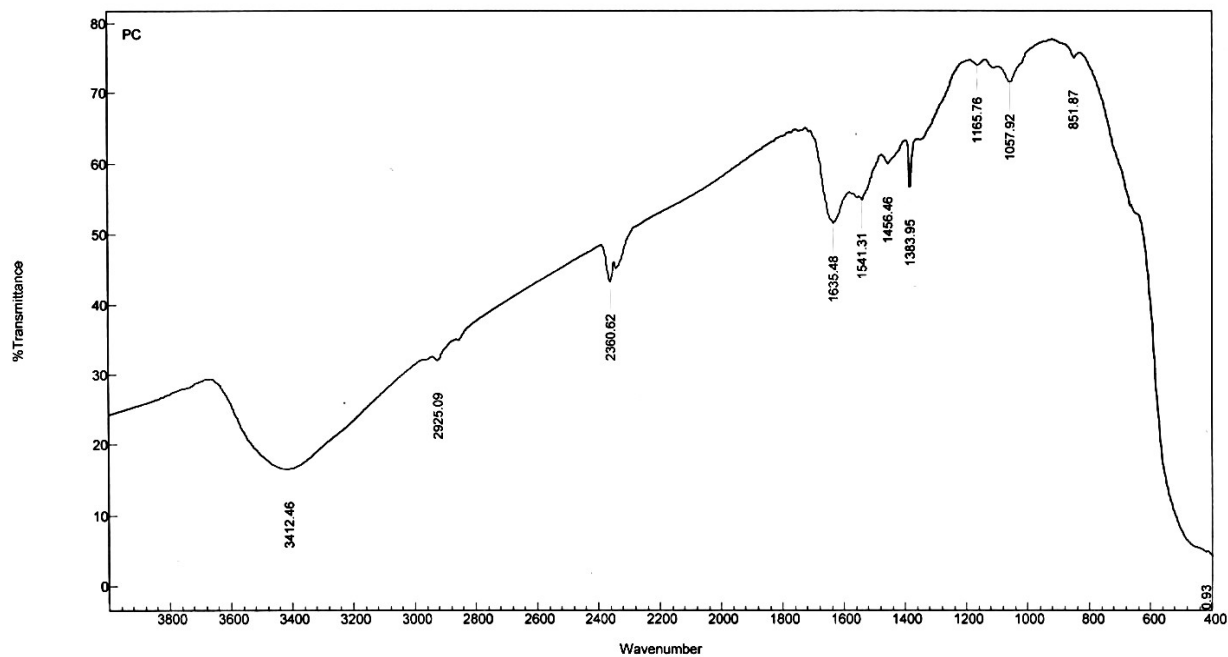
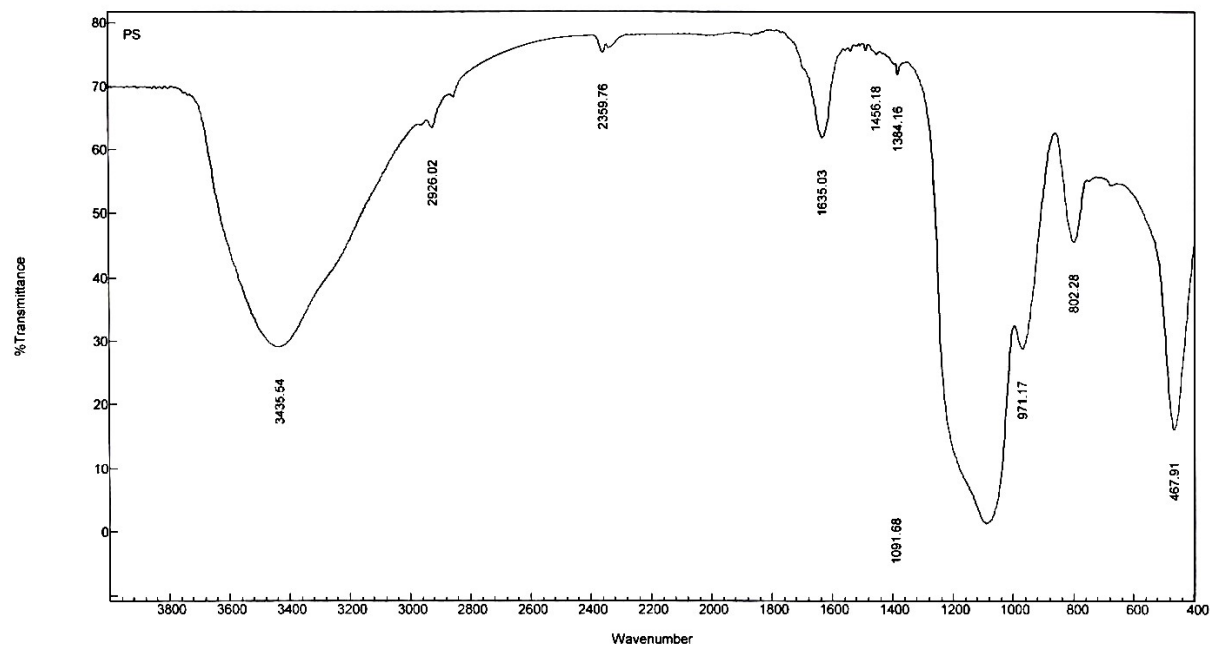
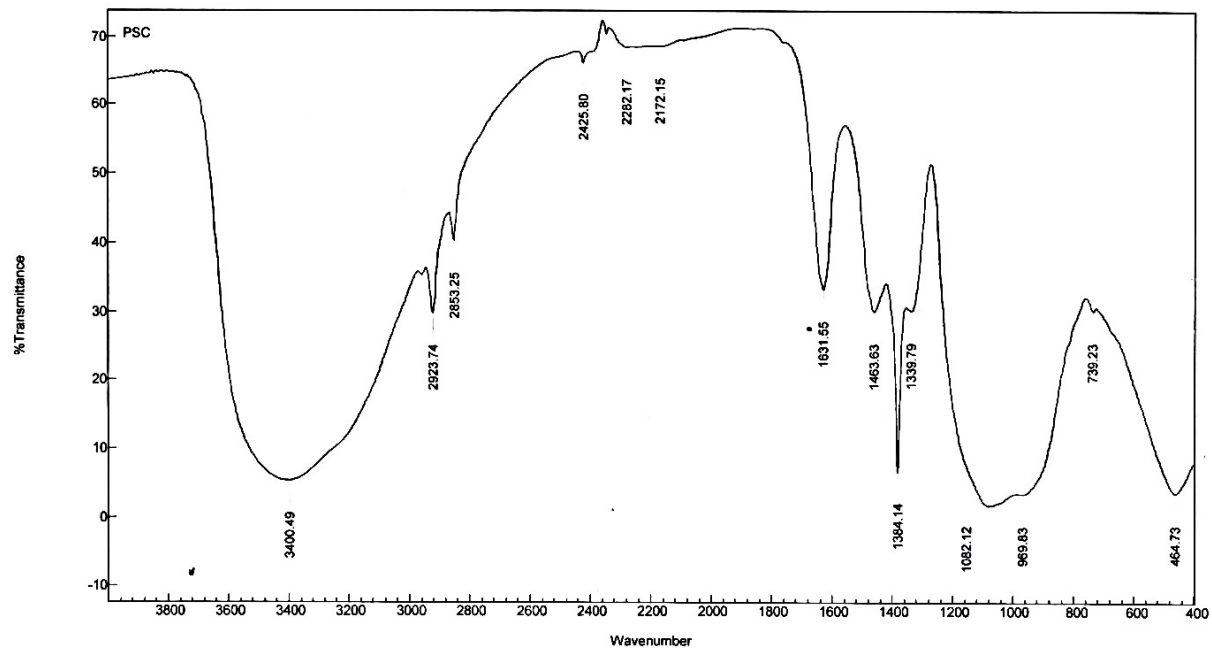


Fig. S1. : FTIR spectra of ceria nanoparticles



Fi

g. S2. : FTIR spectra of silica nanoparticles



F

ig. S3. : FTIR spectra of Silica-Ceria nanoparticles

Fig. S4 shows the EDX result corresponding to ceria nanoparticles that confirm the presence of cerium and oxygen in the entire sample. EDX result of pure silica spheres confirms the presence of Si and O in the material as shown in Fig. S5.

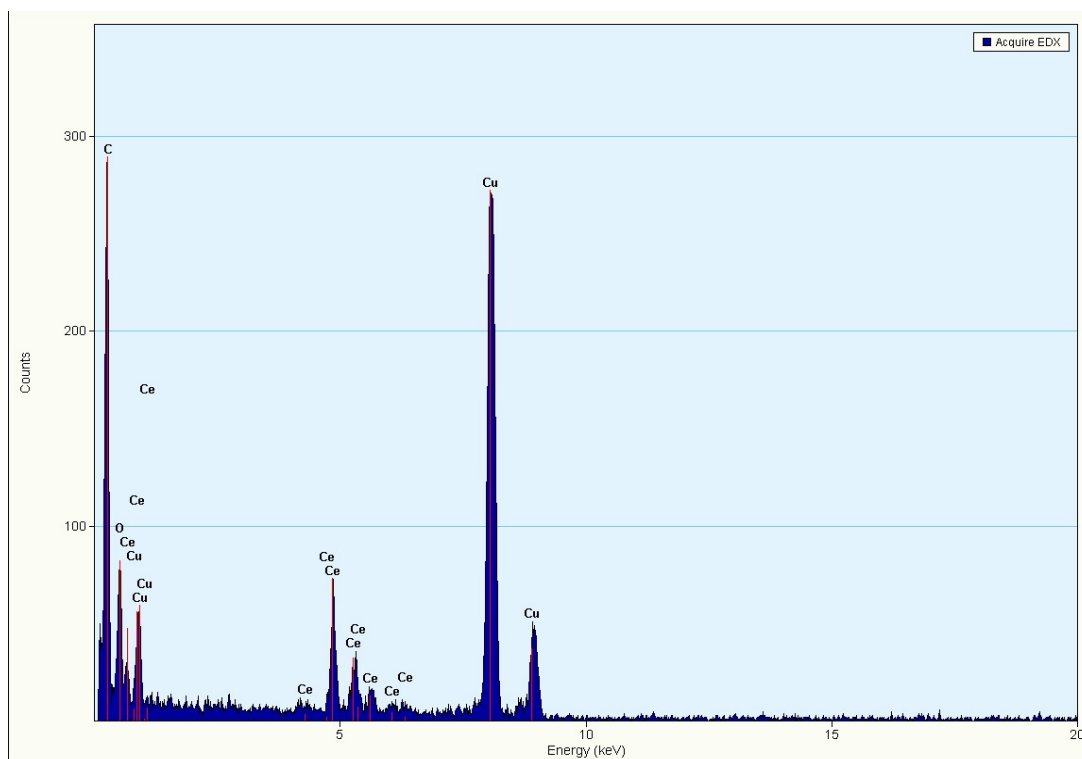


Fig. S4. : EDX data of CeO₂ nanoparticles.

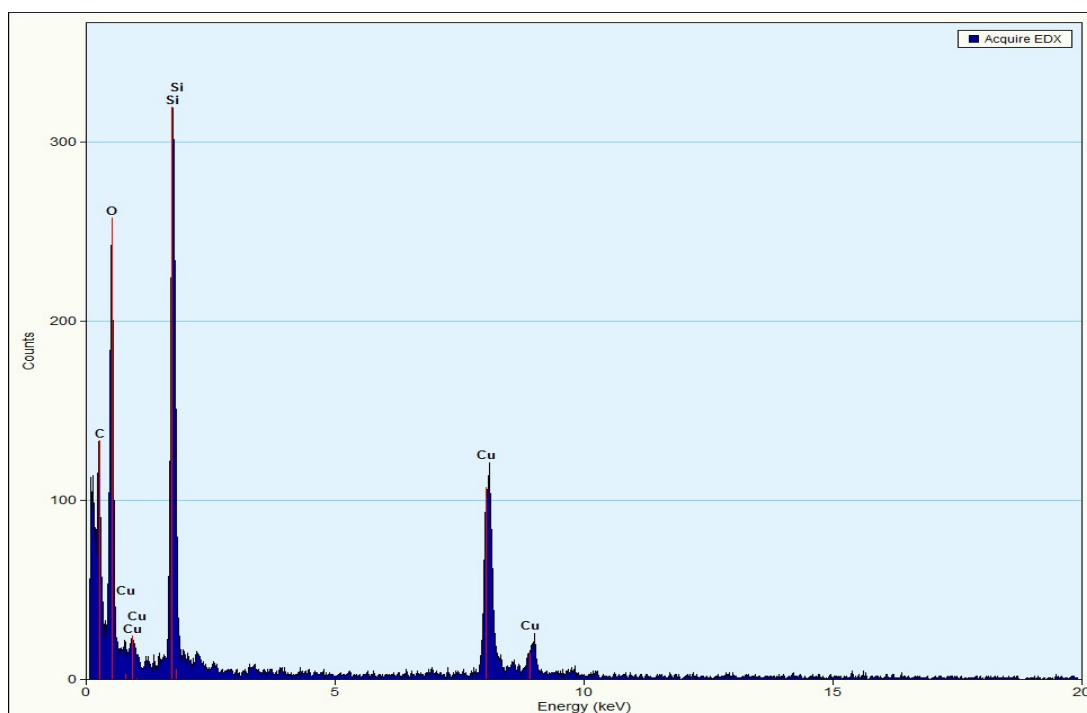


Fig. S5. : EDX data of SiO₂ spheres.

In Fig. S6, the FT-IR ex-situ pyridine absorption spectra of the SiO₂-CeO₂ catalyst show different acidic sites on the surface of the composite material. The FT-IR vibration band due to the Bronsted acid site appears at 1541 cm⁻¹ whereas a band observed at 1456 cm⁻¹ is due to the Lewis acid site of the catalyst. The pyridine absorption study indicates that the reaction proceeds in the influence of Lewis acidic site as well as Bronsted acidic site on the catalyst surface ⁵

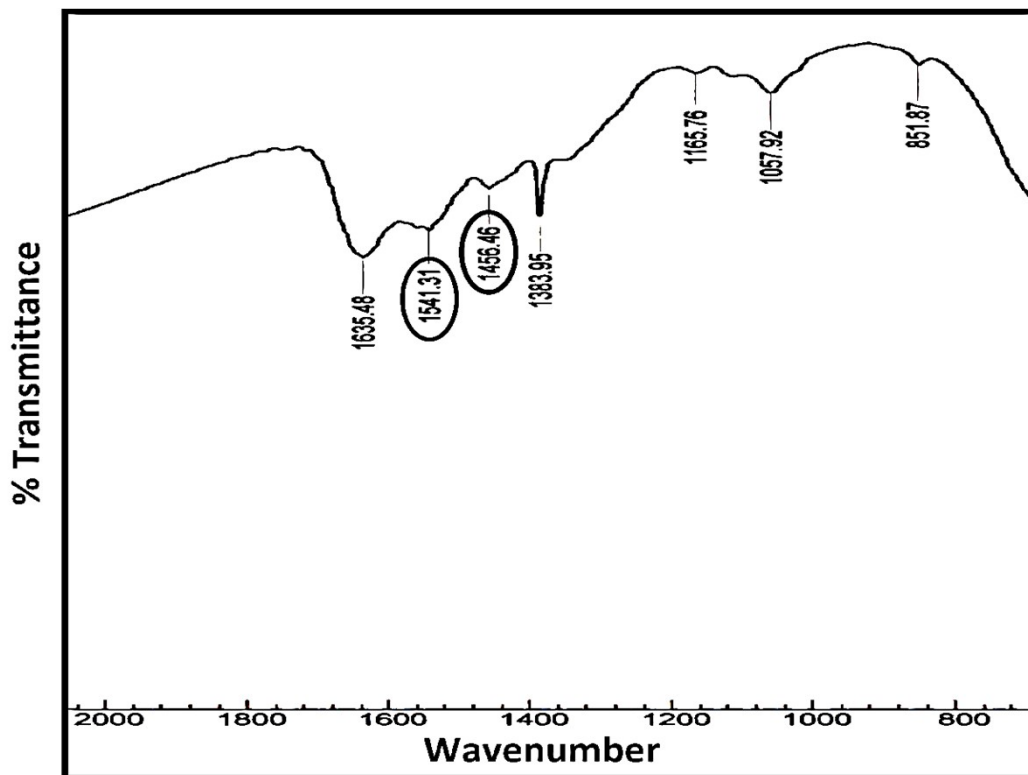


Fig. S6. : The FT-IR pyridine absorption spectra of the SiO₂-CeO₂ catalyst

The LC-MS analysis of liquid products obtained after catalysis using SiO₂-CeO₂ nanocomposite at 120 °C for 1 h, 2 h, and 3 h are shown in Fig. S7, S8, and S9 respectively. The peak obtained in the range of 156 to 158 m/z shows the formation of the product, N-heptyl acetamide after transamidation reaction catalyzed by SiO₂-CeO₂ nanocomposite at different reaction parameters provided.

Acquisition Parameter

Source Type	ESI	Ion Polarity	Positive	Set Nebulizer	0.3 Bar
Focus	Active	Set Capillary	4500 V	Set Dry Heater	190 °C
Scan Begin	50 m/z	Set End Plate Offset	-500 V	Set Dry Gas	4.0 l/min
Scan End	1500 m/z	Set Collision Cell RF	100.0 Vpp	Set Divert Valve	Source

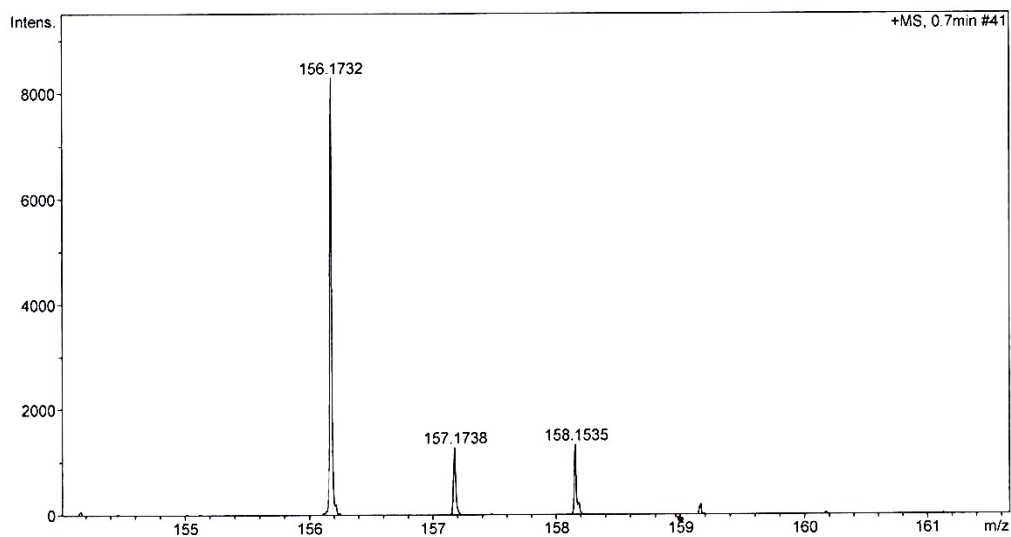
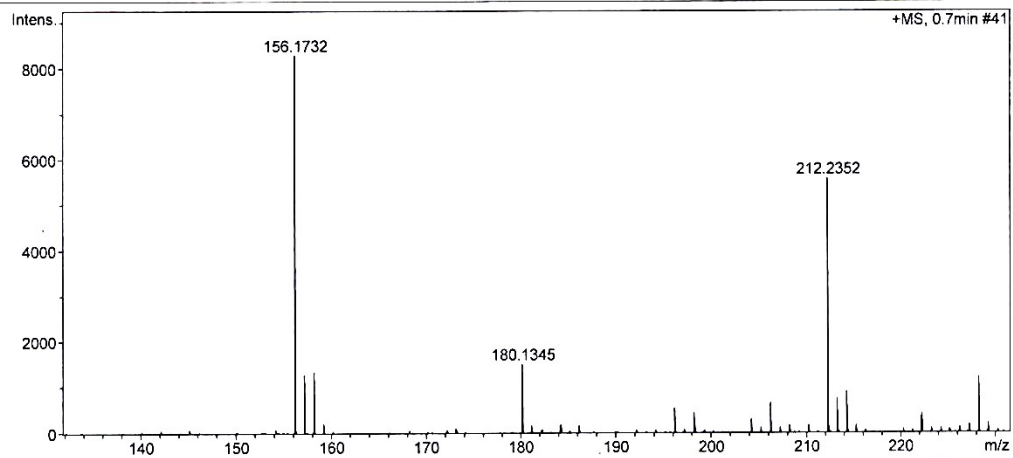


Fig. S7. : LC-MS analysis of liquid products obtained after catalysis using SiO₂-CeO₂ nanocomposite for 120 °C, 1 h.

Acquisition Parameter

Source Type	ESI	Ion Polarity	Positive	Set Nebulizer	0.3 Bar
Focus	Active	Set Capillary	4500 V	Set Dry Heater	190 °C
Scan Begin	50 m/z	Set End Plate Offset	-500 V	Set Dry Gas	4.0 l/min
Scan End	1500 m/z	Set Collision Cell RF	100.0 Vpp	Set Divert Valve	Source

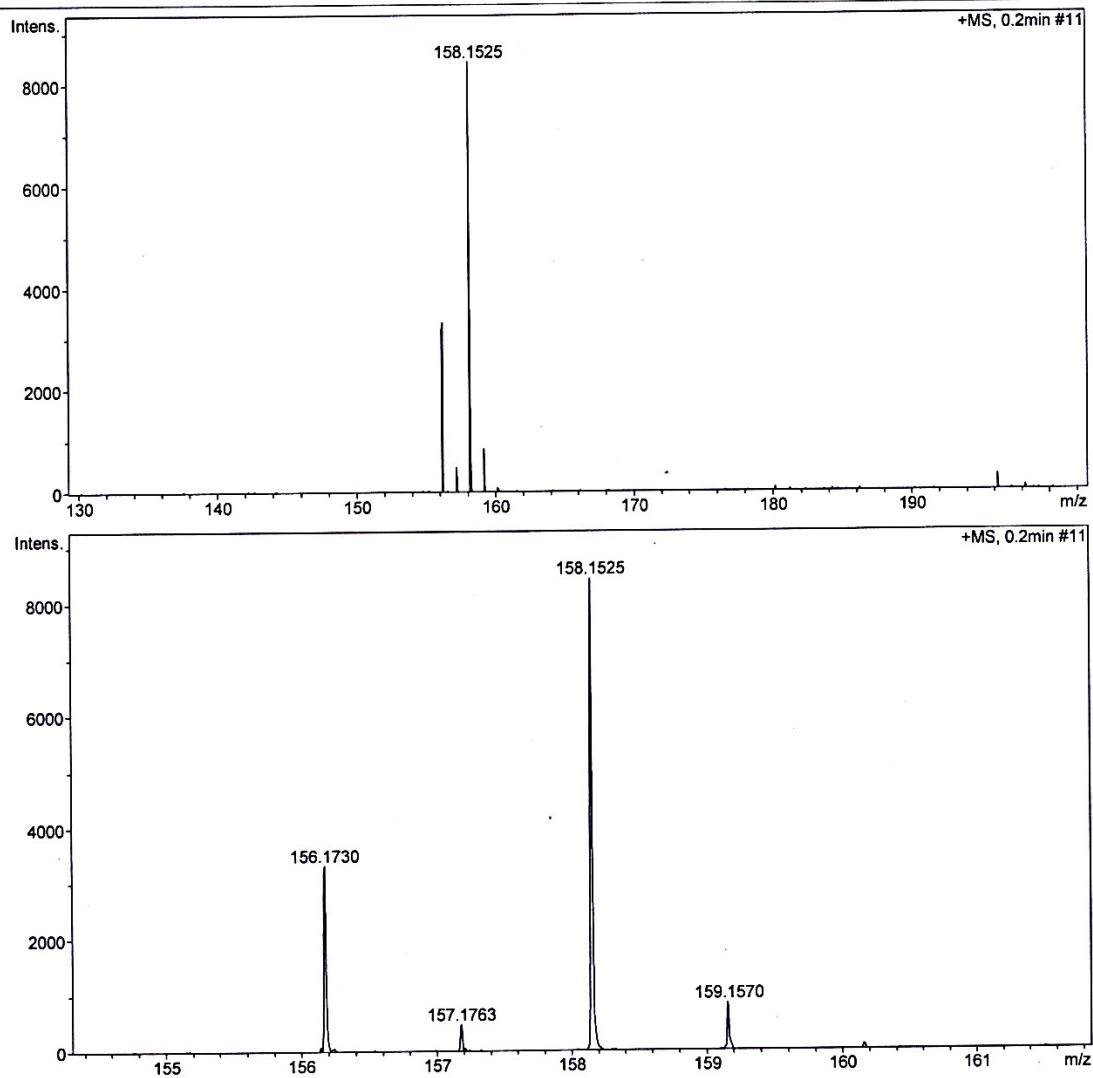


Fig. S8. : LC-MS analysis of liquid products obtained after catalysis using SiO₂-CeO₂ nanocomposite for 120 °C, 2 h.

Acquisition Parameter

Source Type	ESI	Ion Polarity	Positive	Set Nebulizer	0.3 Bar
Focus	Active	Set Capillary	4500 V	Set Dry Heater	190 °C
Scan Begin	50 m/z	Set End Plate Offset	-500 V	Set Dry Gas	4.0 l/min
Scan End	1500 m/z	Set Collision Cell RF	100.0 Vpp	Set Divert Valve	Source

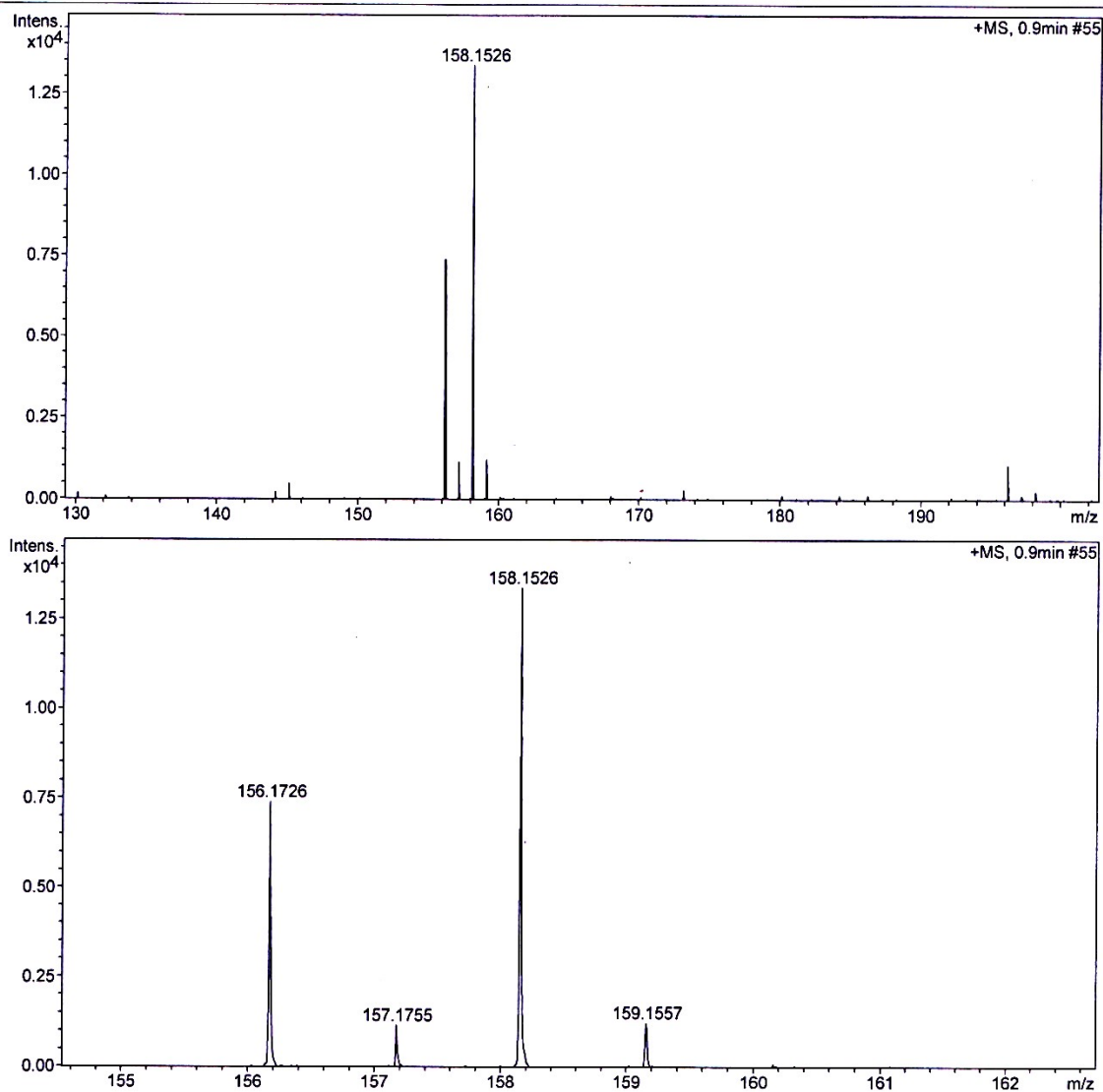


Fig. S9. : LC-MS analysis of liquid products obtained after catalysis using SiO₂-CeO₂ nanocomposite for 120 °C, 3 h.

The transamination reaction was also studied using N-hexyl amine in the presence of acetamide. 50 mg of catalyst was used in each reaction at a temperature of 150 °C for a 3 h period. When using SiO₂ and CeO₂ as catalysts, no activity or conversion was observed. Meanwhile, the catalytic

activity of SiO₂-CeO₂ catalyst in the presence of N-hexyl amine and acetamide was observed to be ~ 80 %. The results are presented in Table No S1.

Table S1. : Catalytic activity and % conversion of reactants in the presence of SiO₂, CeO₂, and SiO₂-CeO₂ nanoparticles as catalysts.

Catalyst	Amide	Amine	Temperature	Time	% Conversion	Selectivity
CeO ₂	Acetamide	N-hexyl amine	150 °C	3 h	0	0
SiO ₂	Acetamide	N-hexyl amine	150 °C	3 h	0	0
SiO ₂ -CeO ₂	Acetamide	N-hexyl amine	150 °C	3 h	80	>99

The PXRD patterns of fresh SiO₂-CeO₂ catalyst and recycled SiO₂-CeO₂ catalyst after 4 catalytic cycles are presented in Fig. S10. The recycled catalyst was calcined at 300 °C before characterization using XRD. All the peaks present in the fresh catalyst were also present in the recycled catalyst with reduced intensities which indicates that the catalyst has undergone little changes during the catalytic process and is stable. Thus, the catalyst can be reused multiple times. TEM images of the recycled catalyst after 4 cycles are also shown in Fig. S11. Spherical-shaped ceria nanoparticles can be seen dispersed in the silica matrix indicating the stability of the catalyst.

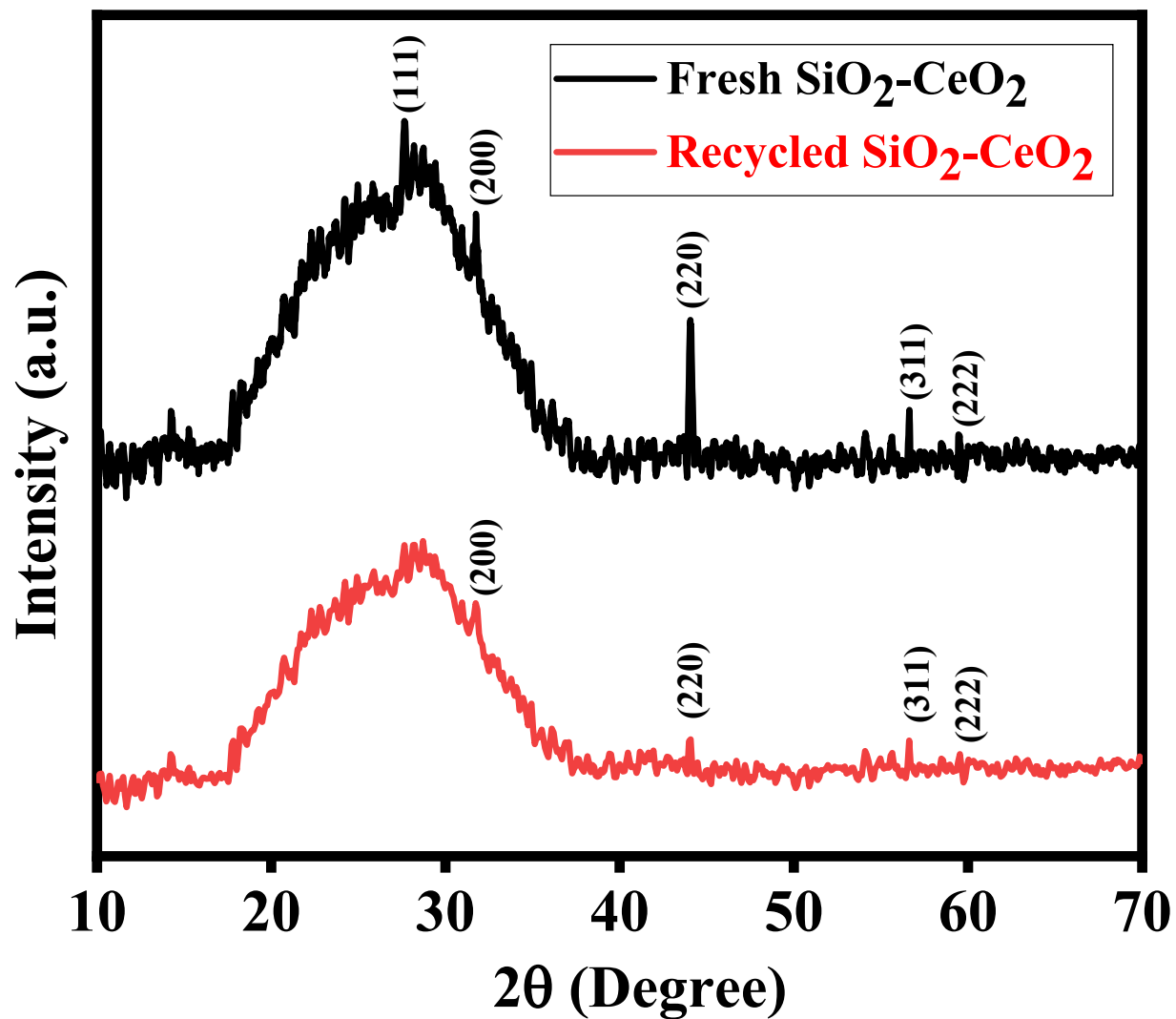


Fig. S10. : XRD patterns of fresh SiO₂-CeO₂ nanocomposite and recycled SiO₂-CeO₂ nanocomposite after 4 cycles.

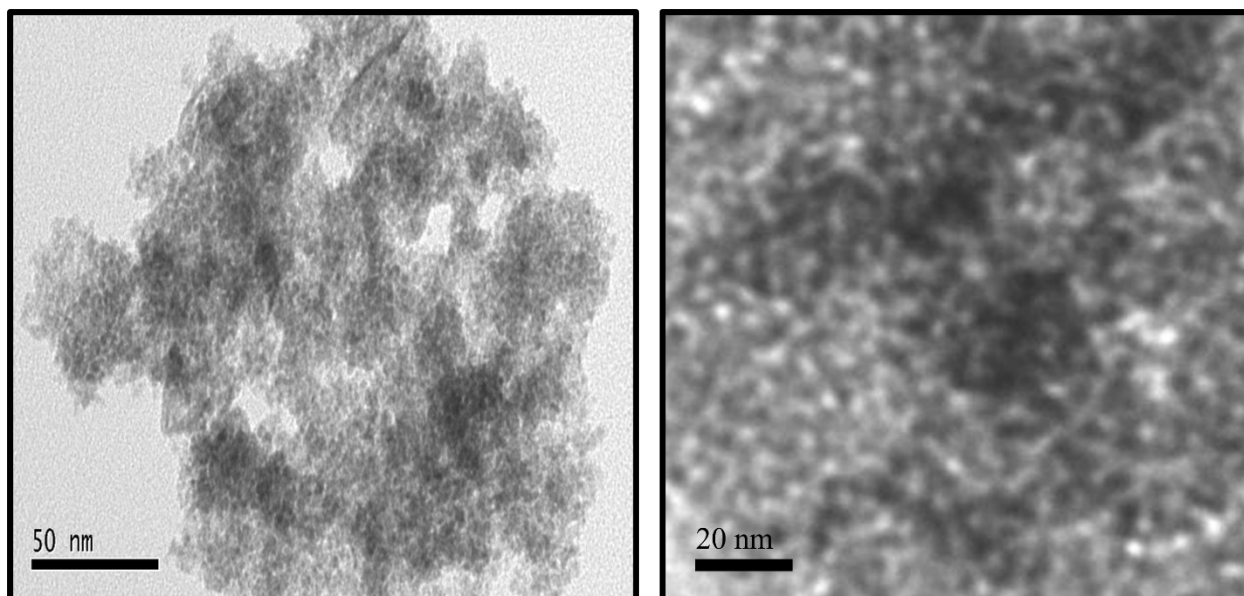


Fig S11. : TEM image of SiO₂-CeO₂ catalyst after 4 catalytic cycles

References

- 1 A. S. Fudala, W. M. Salih and F. F. Alkazaz, *Materials Today: Proceedings*, 2022, **49**, 2786–2792.
- 2 S. Mirfakhraee, R. Bafkary, Y. H. Ardakani and R. Dinarvand, *Journal of Nanoparticle Research*, 2022, **24**, 100.
- 3 E. Salimi and A. K. Nigje, *Carbohydrate Polymers*, 2022, **298**, 120077.
- 4 X. Wen, *RSC Advances*, 2019, **9**, 13908–13915.
- 5 V. Zholobenko, C. Freitas, M. Jendrlin, P. Bazin, A. Travert and F. Thibault-Starzyk, *Journal of Catalysis*, 2020, **385**, 52–60.